

Al₂O₃/ZrO₂복합체의 기계적 물성 및 파괴거동

홍기곤* · 한동빈

*에너지연구부 내화물연구실
무기재료연구분야 구조세라믹연구실
산업과학기술연구소

Mechanical Properties and Failure Analysis of Al₂O₃/ZrO₂ Composites

*Gigon Hong and Dongbin Han

*Refractories Lab in Energy Department
Structural Ceramics Group in CEramic Division

초 록 Al₂O₃/ZrO₂복합분말에 상용분말을 첨가하여 상압소결법으로 Al₂O₃/ZrO₂복합체를 제조한 후, 밀도, 강도, 경도 및 파괴인성등의 물성을 측정하였으며 미세구조 및 파괴단면도 관찰하였다. 상용분말의 첨가량이 중량비로 50%이하인 경우에는 평균 꺾임 강도가 640 MPa정도로 거의 변화가 없었으며, 50%이상 첨가된 경우에는 강도가 저하되었는데, 이는 미세조직과 관계가 있는 것으로 생각된다. 또한 파괴인성(4.3-5.3 Mpam^{1/2}) 낮은 상용분말 첨가량에 비례하여 증가하였다. 파괴단면 관찰 결과 파괴원인으로는 가공에서 생기는 표면 결함, ZrO₂ agglomeration에 의한 crack-like void 및 Al₂O₃/ZrO₂ nano복합체 분말과 상용분말간의 소결성 차이에서 생기는 계면 분리등이 관찰되었는데, nano 복합 분말만을 사용한 소결체에서는 가공에 의한 표면 결함만이 파괴원으로 작용하였다. 또한, 파괴형태는 주로 transgranular fracture이었다.

Abstract Al₂O₃/ZrO₂ composites were fabricated by pressureless sintering from commercial powders and/or nano composite powder of Al₂O₃/ZrO₂. The properties of the composites such as density, strength, hardness and fracture toughness were evaluated. Microstructures and fracture surfaces were also examined.

The flexural strength remains unchanged (~640 MPa) as long as the content of commercial powders is not extremely high, and depends on microstructures of the composites. Fracture toughness(4.3-5.3 MPa · m^{1/2}) increases with increasing content of commercial powders.

Fractography shows that failure-initiating sources are 1) surface flaws resulting from machining damage, 2) crack-shaped voids formed due to ZrO₂ agglomeration, and 3) surface separation caused by inhomogeneous blending and by sinterability difference between nano composite powder and commercial powders of Al₂O₃/ZrO₂. Failure mode of the composites was mainly transgranular.

I. Introduction

Hot-pressing method has been mainly used to fabricate dense and fine grain ZTA(ZrO₂-Toughened Al₂O₃) ceramics. Mechanical properties such as fracture toughness and strength have been reported in a number of papers, but the relationship of mechanical properties and fracture behavior of ZTA ceramics fabricated from pressureless sintering¹⁾ has been rarely

studied.

Since Engle and Hubner²⁾ initiated a systematic study relating strength to processing variables, Lange et al.³⁻⁵⁾ examined processing-related fracture origins of Al₂O₃/ZrO₂ composites and obtained the following results : Internal, crack-like surfaces responsible for the much-lower strength are located at the fracture origins of sintered materials of Al₂O₃/ZrO₂ composite system, which are mainly pro-

duced by the different sinterability of large agglomerates relative to their surroundings in the powder compact. The ZrO₂ agglomerates shrank away from consolidated Al₂O₃/ZrO₂ powder matrix during sintering and crack-like voids accounted for strength degradation.

Slurry/filtration route⁶⁾, CVD method⁷⁾, and sol-gel method⁸⁻⁹⁾ were investigated to preclude agglomeration of ZrO₂ powders and to fabricate Al₂O₃/ZrO₂ composites with uniform microstructures, but these methods have disadvantages such as complex and/or costly manufacturing processes.

This paper reports mechanical properties and failure analysis of Al₂O₃-15 vol% ZrO₂(+3 mol% Y₂O₃) composites fabricated from pressureless sintering, where commercial Al₂O₃ and Y-TZP powders were added to Al₂O₃/ZrO₂ nano composite powder prepared by co-precipitation method.

II. Experimental procedures

Materials used to prepare Al₂O₃/ZrO₂ system contains 15 vol% ZrO₂(+3 mol% Y₂O₃) in this study.

Tetragonal ZrO₂ is retained by the constraint of Al₂O₃ matrix and the addition of Y₂O₃ at sintering temperatures of Al₂O₃/ZrO₂ composites¹⁰⁾, and is a significant toughening agent.¹¹⁾

Nano composite powder of Al₂O₃-15 vol% ZrO₂(+3 mol% Y₂O₃) was prepared by co-precipitation of the common solution of Al₂(SO₄)₃ · 18H₂O, ZrOCl₂ · 8H₂O and YCl₃ · 6H₂O with NH₄OH at the pH=7, and followed by calcination of coprecipitated metal hydroxides at 1250 °C for 1hr.¹²⁾ The average particle size and specific surface area of the nano composite powder was 0.87 μm and 15 m²/g, respectively.¹²⁾

Transmission electron microscopy(TEM) was used for a more detailed observation of the powder microstructures, e.g., the morpholo-

gy of Al₂O₃ particles and the dispersion state of ZrO₂ particles. Also, thin-foil energy dispersive X-ray spectroscopy(EDS) analysis using finely focused electron beams (~8 to 50nm) in TEM was employed to distinguish Al₂O₃ from ZrO₂ particles.

Composite powders for sintering were prepared by mixing the appropriate amounts of submicrometer-sized commercial Al₂O₃*, ZrO₂(+3 mol% Y₂O₃)** powders and nano composite powder in alcohol. The mixed composite powders were dried by rotary distillation. The mixtures were uniaxially(25 MPa) and isostatically presses(138 MPa) prior to sintering at 1650 °C for 2hr in air.

This sintered composites were cut into rectangular bars(3X6X33mm) for 3-point flexural test(cross head speed : 0.5mm/min, span : 2.54cm). All bar specimens were polished with diamond paste down to 1 μm of roughness to preclude surface defects as much as possible.

Microstructures of the composites were examined in the back-scattered mode of the scanning electron microscope(SEM) after thermal etching at 1450 °C for 1hr. Failure mode and failure-initiating sources were observed on as-fractured surfaces in the secondary mode of SEM.

The values of fracture toughness were measured by the indentation method using the following equation.¹³⁾

$$\frac{K_{IC}}{Ha^{1/2}} = 0.203(C/a)^{-3/2}$$

Where H is the hardness, a the impression radius and C the radial/median crack length.

III. Results and Discussion

Figure 1 shows morphology of Al₂O₃/ZrO₂ nano composite powder observed by high resolution TEM. ZrO₂ particles with 25-50nm sizes are homogeneously dispersed at the inner and outer parts of Al₂O₃ particles. ZrO₂ parti-

* Alcoa A-16, Aluminum Company of America, Pittsburg, PA.

** HSY-3.0, Daichi-Kigenso, Tokyo, Japan. (Average particle size : 0.5 μm)

Table I. Properties of Al₂O₃/ZrO₂ Composites

Material	Content of Commercial Powders*(wt.%)	Sintered Density (% theoretical)**	Flexural Strength (MPa)	Hardness (GPa)	Fracture Toughness (MPa m ^{1/2})
ZTA0	0	97.5	637 ± 30	10.9 ± 0.5	4.3 ± 0.7
ZTA10	10	97.7	640 ± 20	10.0 ± 0.7	4.8 ± 0.6
ZTA30	30	98.0	630 ± 25	11.3 ± 0.9	4.8 ± 1.0
ZTA50	50	98.8	641 ± 30	12.6 ± 0.8	5.2 ± 0.8
ZTA80	80	99.0	530 ± 50	12.9 ± 0.8	5.3 ± 0.8

* Composition of commercial powders : Al₂O₃ - 15 vol% ZrO₂ (+ 3 mol% Y₂O₃)

** $\rho_{\text{Al}_2\text{O}_3} = 3.98 \text{ g/cm}^3$, $\rho_{\text{ZrO}_2} = 6.08 \text{ g/cm}^3$

In all composites, tetragonal ZrO₂ was retained above 95% after polishing.

In all composites, tetragonal ZrO₂ was retained in the range of 75-80% after fracture.

cles existing in inside of Al₂O₃ particles are lens shape. It may be considered that the former and the latter are under equiaxial and anisotropic compressive stress of Al₂O₃ particles, respectively.

Table I shows properties of Al₂O₃/ZrO₂ composites. The densities of the composites were more than 97% of theoretical density. The more the content of commercial powders increases, the higher the densities become. Lange and Hirlinger¹⁴⁾ reported that Al₂O₃/ZrO₂ interfacial energy is lower than Al₂O₃ grain boundary energy, which suggests that the formation of Al₂O₃/ZrO₂ interfaces would increase the driving force for densification. Also, Kibbel and Heuer¹⁵⁾ have that intergranular ZrO₂ particles grow faster than intragranular particles does, despite their initially larger size; the kinetics of particle growth are clearly faster on the grain boundaries than within Al₂O₃ grains.

As shown in Figure 1, the increased content of Al₂O₃/ZrO₂ nano composite powder increases the number of Al₂O₃/ZrO₂ interfaces and intragranular ZrO₂ particles (smaller than intergranular and commercial ZrO₂ particles). Thus, with increasing the content of commercial powders, high density of the composites is shifted toward higher fractions under the same sintering condition.

The flexural strength remains unchanged (~ 640MPa) as long as the content of commercial powders is not extremely high, and depends on microstructures of the composites. The effects of microstructures on strength can be explained in Figure 2. At the extremely high content of commercial powders shown on Figure 2 (B), the ZrO₂ particles (white) was ineffective in pinning the Al₂O₃ readily occurred. At the lower weight fractions, shown in Figure 2 (A), the ZrO₂ particles are uniformly located at the Al₂O₃ grain boundaries, effectively limiting the Al₂O₃ grain size. Therefore, even though the starting powders are the same composition, there must be difference in ZrO₂ particle-limited grain growth occurred during sintering, depending on starting powders.

Table I shows close relationship between hardness and density, where higher hardness was accompanied by density increase.

Fracture toughness increases with increasing content of commercial powders. It can be explained by Figure 3 showing microcracking of the composites around indentation crack. At the higher weight fractions, such as shown on Figure 3(B), large ZrO₂ particles remain at the Al₂O₃ grain boundaries and they effectively absorb crack propagation energy by stress-induced phase transformation or crack deflection. At the lower weight fractions, small ZrO₂

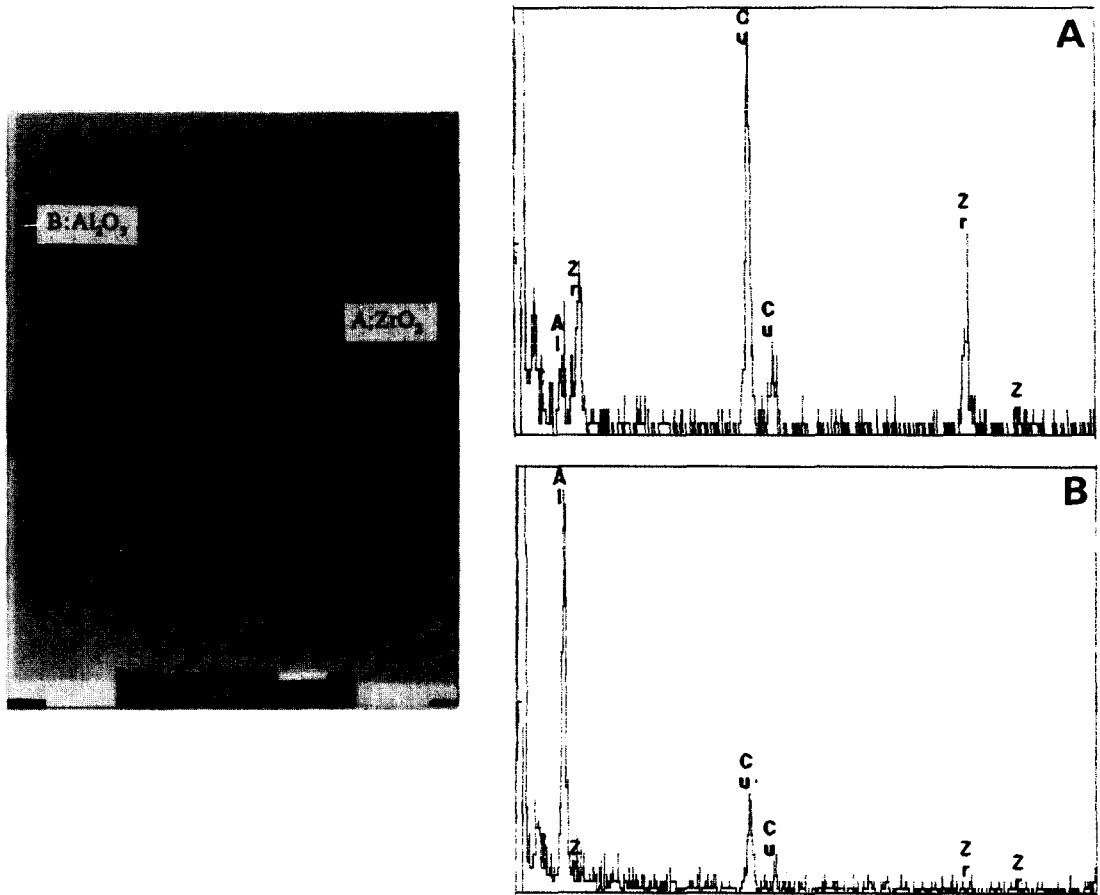


Fig. 1. Transmission electron micrograph and energy dispersive X-ray spectra $\text{Al}_2\text{O}_3/\text{ZrO}_2$ nano composite powder. [Cu detected due to copper grid]

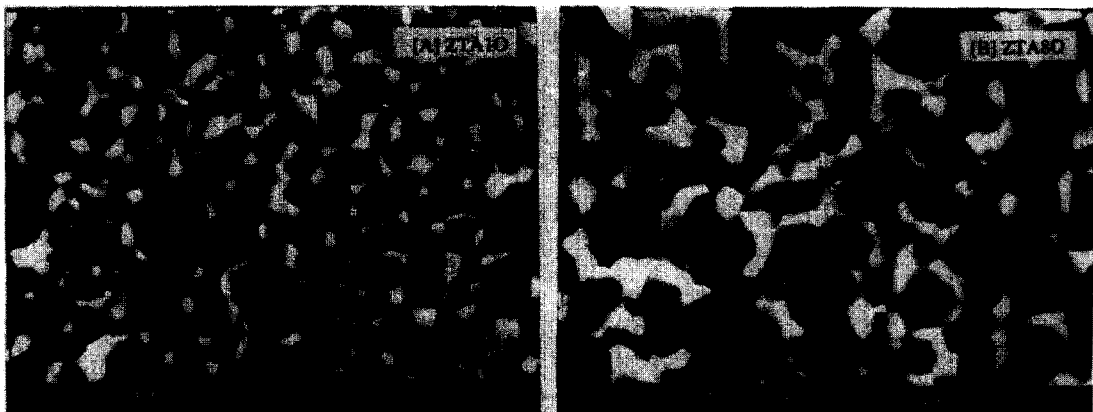


Fig. 2. The back-scattered scanning electron micrographs showing microstructures of $\text{Al}_2\text{O}_3/\text{ZrO}_2$ composites.

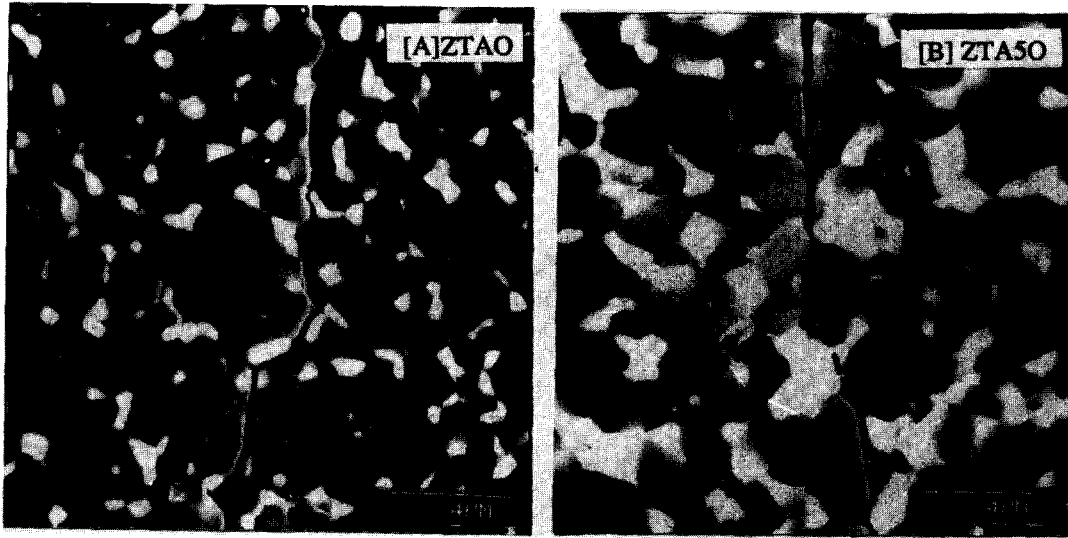


Fig. 3. The back-scattered scanning electron micrograph showing microstructures of $\text{Al}_2\text{O}_3/\text{ZrO}_2$ composites around indentation crack.



Fig. 4. Scanning electron micrographs of fracture surfaces of $\text{Al}_2\text{O}_3/\text{ZrO}_2$ nano composites.

particles are located at the Al_2O_3 grain boundaries, and only small fraction of ZrO_2 absorbs crack propagation energy. In all composites, Al_2O_3 grains showed a transgranular crack produced by a Vickers indenter.

Figure 4 shows the fracture surfaces of the composites. The fracture mode is mainly transgranular, and it agrees with the result observed in Figure 3. Figure 5 to 7 show failure sources of the composites observed in this

study. In the composite prepared from $\text{Al}_2\text{O}_3/\text{ZrO}_2$ nano composite powder alone, the fracture initiates from surface flaws created by machining damage on tensile surface(Figure 5). In the cases of adding commercial powders to $\text{Al}_2\text{O}_3/\text{ZrO}_2$ nano composite powder, crack-shaped voids formed due to ZrO_2 agglomeration and surface separation caused by inhomogeneous mixing and by sinterability difference between $\text{Al}_2\text{O}_3/\text{ZrO}_2$ nano composite powder and commercial powders as well as surface flaws are observed, and these act as factors of strength degradation(Figure 6). Especially, Figure 7 illustrates the morphology of a less-typical failure source and a matching hole was observed on the other side of the

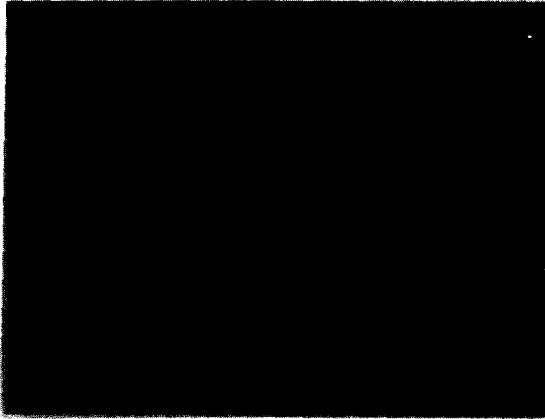


Fig. 5. Scanning electron micrograph of a fracture origin of ZTAO.

fractured surface. Because of Al_2O_3 and ZrO_2 existing together, failure source is not formed due to ZrO_2 agglomeration like Figure 6. Also, in contrast to the fracture mode of Figure 4, the fracture mode within the hole(failure source) is intergranular.

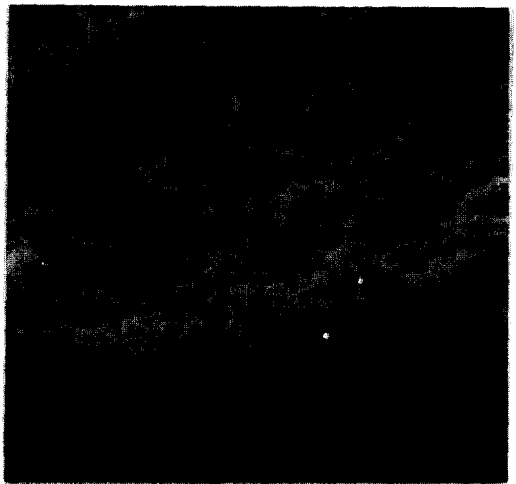
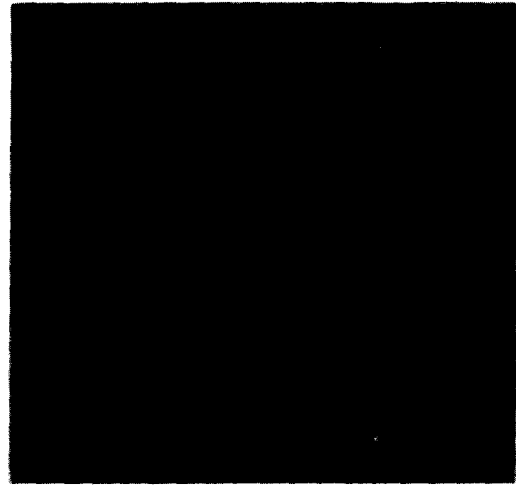


Fig. 6. Scanning electron micrograph of a fracture origin of ZTA30 with different magnitude.

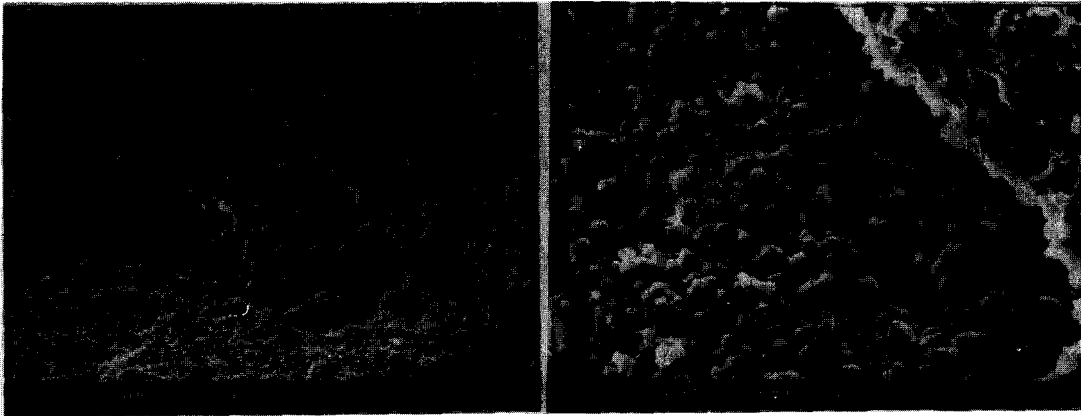


Fig. 7. Scanning electron micrograph of a fracture origin of ZTA80 with different magnitude.

IV. Summary

The flexural strength remains unchanged (~ 640 MPa) as long as the content of commercial powders is not extremely high, and depends on microstructures of the composites. Fracture toughness ($4.3\text{--}5.3\text{MPa} \cdot \text{m}^{1/2}$) increases with increasing content of commercial powders.

Fractography showed that failure-initiating sources in $\text{Al}_2\text{O}_3/\text{ZrO}_2$ composites are surface flaws, crack-shaped voids and surface separation. Fracture mode of the composites are also mainly transgranular.

Crack-shaped voids and surface separation are not observed in the composite fabricated from $\text{Al}_2\text{O}_3/\text{ZrO}_2$ nano composite powder alone. Thus, it is considered that it can be used as a reliable high-tech $\text{Al}_2\text{O}_3/\text{ZrO}_2$ composite, if its sinterability is somewhat improved.

REFERENCES

1. S.R. Witek and E.P. Butler, "Zirconia Particle Coarsening and the Effects of Zirconia Additions on the Mechanical Properties of Certain Commercial Aluminas," *J. Am. Ceram. Soc.*, 69(7) 523-529(1986).
2. V. Engle and H. Hubner, "Strength Improvement of Cemented Carbides by Hot Isostatic Pressing," *J. Mater. Sci.*, 13(9) 2003-2013(1978).
3. F.F. Lange, "Processing-Related Fracture Origins : I, Observations in Sintered and Isostatically Hot-Pressed $\text{Al}_2\text{O}_3/\text{ZrO}_2$ Composites," *J. Am. Ceram. Soc.*, 66(6) 396-398(1983).
4. F.F. Lange and M. Metcalf, "Processing-Related Fracture Origins : II, Agglomerate Motion and Cracklike Internal Surfaces Caused by Differential Sintering," *J. Am. Ceram. Soc.*, 66(6) 398-406(1983).
5. F.F. Lange, B.I. Davis and I.A. Aksay, "Processing-Related Fracture Origins : III, Differential Sintering of ZrO_2 Agglomerates in $\text{Al}_2\text{O}_3/\text{ZrO}_2$ Composites," *J. Am. Ceram. Soc.*, 66(6) 407-408(1983).
6. F.F. Lange, T. Yamaguchi, B.I. Davis and P.E.D. Morgan, "Effect of ZrO_2 Inclusions on the Sinterability of Al_2O_3 ," *J. Am. Ceram. Soc.*, 71(6) 446-448(1988).
7. S. Hori, M. Yoshimura, S. Somiya, R. Kurita and H. Kaji, "Mechanical Properties of ZrO_2 -Toughened Al_2O_3 Ceramics from CVD Powders," *J. Mater. Sci. Letter*, 4, 413-416(1985).
8. P.F. Becher, "Transient Thermal Stress Behavior in ZrO_2 -Toughened Al_2O_3 ," *J.*

- Am. Ceram. Soc., 64(1) 37-39(1981).
9. A.H. Heuer, N. Claussen, W.M. Kriven and M. Ruhle, "Stability of Tetragonal ZrO_2 Particles in Ceramic Matrices," J. Am. Ceram. Soc., 65(12) 642-650(1982).
 10. T. Arahori, N. Iwamoto and N. Umesaki, "Influence of Y_2O_3 Addition on the Transformation Behavior of ZrO_2 in Al_2O_3 - ZrO_2 Composites," *Yogyo-Kyokai-Shi*, 95(10) 949-954(1987).
 11. F.F. Lange, "Transformation Toughening, Parts 1, 2, 3, 4, 5" J. Mater. Sci., 17, 235-254(1982).
 12. Gigon Hong and Honglim Lee, "Properties of Al_2O_3 -15 vol%/ ZrO_2 (+3mol% Y_2O_3) Powder Prepared by a Co-Precipitation Method," J. Kor. Ceram. Soc., 26(2) 210-220(1989).
 13. K. Niihara, N. Nakahira and T. Hirai, "The Effect of Stoichiometry on Mechanical Properties of Boron Carbide," J. Am. Ceram. Soc., 67(1) C13-G14(1984).
 14. F.F. Lange and M.M. Hirlinger, "Hindrance of Grain Growth in Al_2O_3 by ZrO_2 Inclusions," J. Am. Ceram. Soc., 67(3) 164-168(1984).
 15. B.W. Kibbel and A.H. Heuer, "Ripening of Inter- and Intragranular ZrO_2 Particles in ZrO_2 -Toughened Al_2O_3 ," pp. 415-424 *Advances in Ceramics*, Vol. 12. Edited by A.H. Heuer and L.W. Hobbs, The American Ceramic Society, Columbus, OH, 1981.